International Journal of Control and Automation
Vol. 11, No. 2 (2018), pp.115-124
http//dx.doi.org/10.14257/ijca.2018.11.2.10

Analysis of Inter-Carrier Interference by Closed-Loop Phase Noise on OFDM Systems

Jihun Koo

Department of Smart IT, Osan University, Osan, Korea
Jihun.koo@osan.ac.kr

Abstract

This paper shows the analysis and derivations of inter-carrier interference (ICI) caused by closed-loop phase noise on OFDM communication system. The closed loop phase is composed of carrier frequency offset and common phase noise. For realistic result, the closed-loop phase noise is measured using a commercial RF IC. Moreover, the effect of measured phase noise was analyzed in terms of CPE and CFO, respectively, and the SNR degradation due to CPE and CFO were analyzed for OFDM communication system. The analyzed result shows ICI by common phase noise is greater than carrier frequency offset as much as 12.3dB on WLAN system. Also, the maximum phase noise and residual frequency offset for the 10-3 BER are plotted by comparing the analyzed ICI components to the required SNR for each modulation order of IEEE802.11ax

Keywords*: Inter-carrier interference (ICI), common phase error (CPE), carrier frequency offset (CFO)*

1. Introduction

Orthogonal frequency division multiplexing (OFDM) has become increasingly popular for wideband digital communication systems such as wireless local area network (WLAN) and 4G mobile communications due to its robustness under multipath effects. A wireless communication system using OFDM scheme typically works over frequency-selective channels where the use of a cyclic prefix (CP) of adequate length v maintains the orthogonality between the subcarriers and eliminates the inter-symbol interference (ISI). On the other hand, carrier frequency offset (CFO) between transmitter and receiver VCO and common phase error (CPE) caused from phase noise (PN) will cause inter-carrier interference (ICI).

The orthogonality of the consecutive OFDM symbols is maintained by appending a length v cyclic prefix (CP) at the start of each symbol which is transformed by Invers Fast Fourier Transforms (IFFT) of finite length, N. The CP is obtained by taking the last v samples of each symbol and consequently the total length of the transmitted OFDM symbols can be N+v samples. For each OFDM symbol to avoid inter-symbol interference (ISI) or ICI, the length of the channel impulse response (CIR) should be less than v samples. Then, the symbol is transmitted after mixing with carrier frequency generated by transmitter VCO. After passing wireless channel, the receiver frontend mixes it with carrier frequency generated by receiver VCO to make baseband signal. The baseband receiver discards the CP and takes only the last N samples per each OFDM symbol by FFT block [1], [2]. Figure 1 shows the block diagram of the system.

Received (October 19, 2017), Review Result (December 19, 2017), Accepted (January 28, 2018)

ISSN: 2005-4297 IJCA

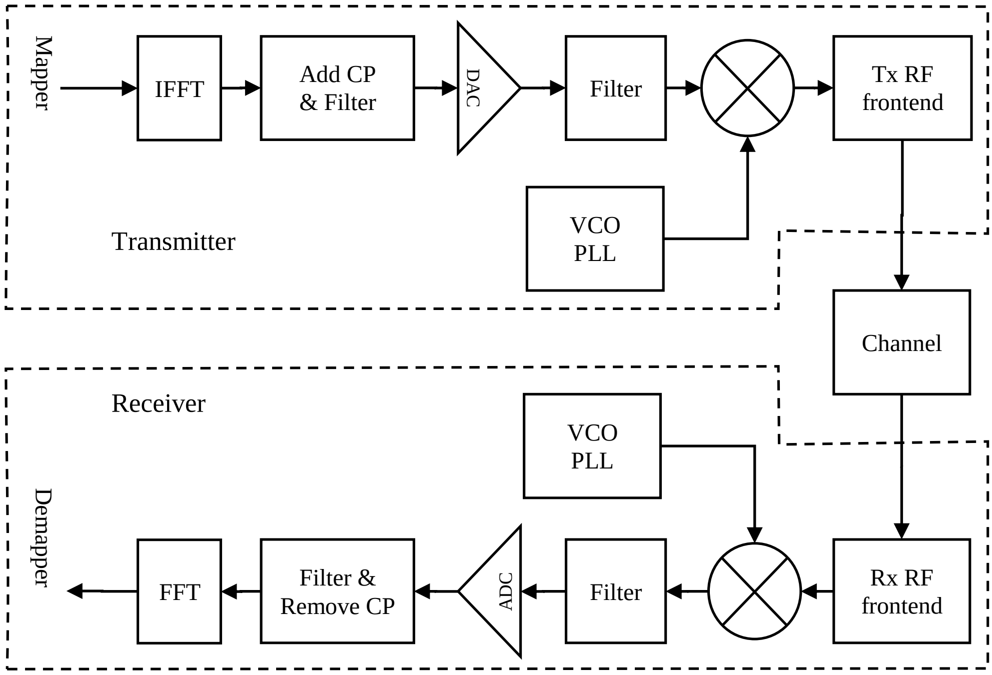

Figure 1. Block Diagram of OFDM Communication System

Unfortunately, OFDM has been proven to be very sensitive to carrier frequency errors composed of CFO and CPE. These random frequency errors in OFDM system distort orthogonality between subcarriers. As a result, inter-carrier interference (ICI) is occurred. And, the undesired ICI degrades the performance of the error vector magnitude (EVM) on transmitter and packet error rate (PER) on receiver.

There have been various works on performance assessment of OFDM with PN, typically focusing on the determination of the statistical properties of the ICI affecting each subcarrier [3], [4], [5]. In [6], the problem of analytically assessing the maximum achievable rates of OFDM transmissions has been considered as well. However, a common feature of all these works is that they do not consider the practical phase noise model. The author in [7] use phase noise model of typical oscillator. But it is also far from closed-loop phase noise characteristics of ICs [8].

In this paper, we analyze ICI for close-loop phase noise in OFDM communication system and predict interference between subcarriers according to modulation order and SNR. In Section II, the phase noise of the WLAN system is modeled based on the experimental results. In Section III, the ICI is divided into the error due to the residual frequency offset component and the error caused by the common-phase noise. . Finally, let's conclude in Chapter IV.

2. Phase Noise Model in WLAN

2.1. One-Pole Phase Noise Model

Firstly, the phase noise model in WLAN is introduced. A one-pole PN model shown in Figure 2 was adopted and used in IEEE 802.11 and is used for wireless performance verification [9].

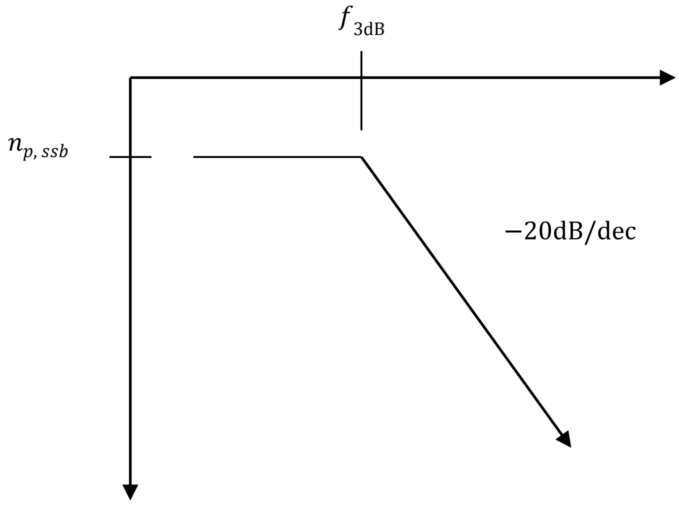

Figure 2. One-Pole Phase Noise Model in WLAN

The transfer function of the one-pole model can be described as below:

$$G(j\omega) = \frac{1}{1 + j\frac{f}{f_{3\mathrm{dB}}}} \tag{1}$$

where, $f_{3\mathrm{dB}}$ is one sided 3-dB bandwidth.

Using the two free parameters, 3 dB cutoff frequency, $f_{3\mathrm{dB}}$ and phase noise in degree $n_{p,degree}$, the phase noise process can be derived as follows:

a) Calculate AWGN phase noise power

$$P_{n,awgn} = \frac{\left(n_{p,degree}\frac{\pi}{180}\right)^2 \cdot f_s}{2EQBW} \tag{2}$$

where equivalent bandwidth $EQBW = \int_0^\infty |G(j\omega)|^2 = f_{3dB} \cdot \pi/2$. And, f_s denotes the sampling frequency.

b) Generate AWGN phase noise $n_{p,awgn} \sim N(0,\ P_{n,awgn})$

c) Calculate Colored Gaussian phase noise using transfer function G.

2.2. Measurement Results of Phase Noise

The phase noise of the MAX2829, a multiple-input and multiple-output (MIMO) WLAN RF transceiver IC fabricated with Maxim Integrated BiCMOS process, was measured to compare the phase noise characteristics generated by the above steps. Its design target for RF & analog is described on [8].

Figure 3 compares the phase noise of the MAX2829 with the phase noise of the one-pole model with f3dB of 100kHz, which is similar to the phase noise model of 0.5 °. Here, since the symbol period in the WLAN is 250 kHz, it can be assumed that the phase noise of the lower frequency can be eliminated using the pilot subcarriers specified in the 802.11 standard. Therefore, when calculating the integrated phase noise (IPN) that affects the receiver, frequencies above 250kHz can be obtained by accumulating. Table 1 shows cumulative phase noise from 250kHz to 40MHz for each root-mean-square degree (0.5 °, 1.0 ° and 1.5 °) in a one-pole phase noise model.

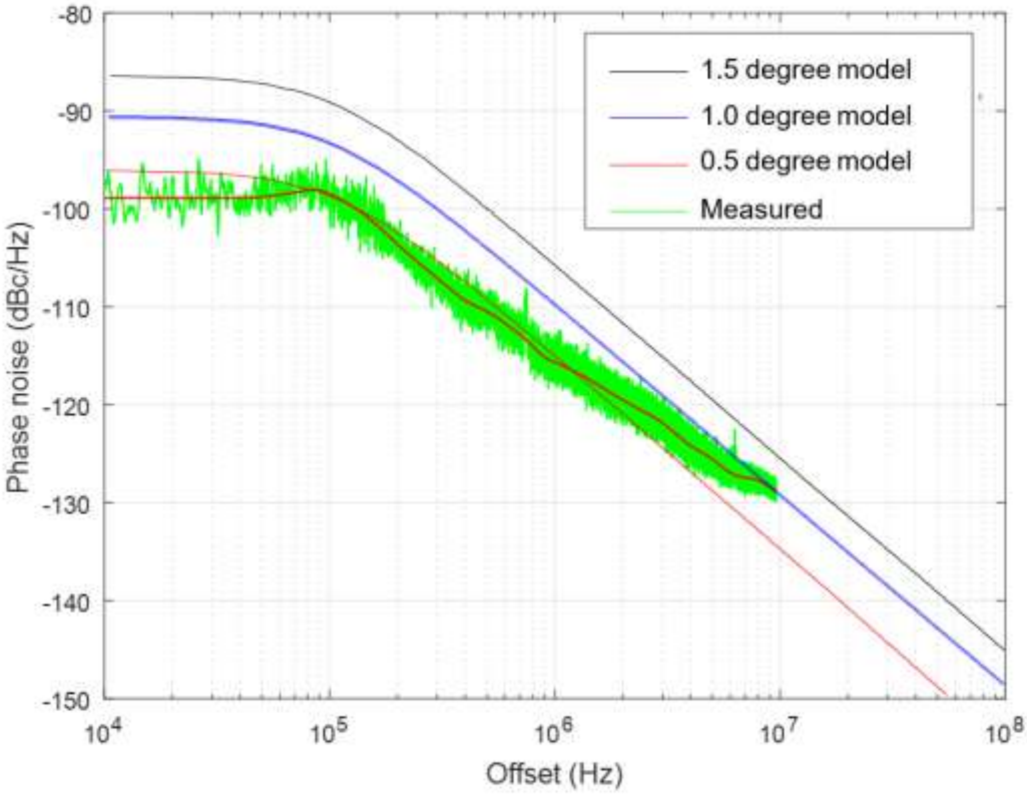

Figure 3. Phase Noise of MAX2829 Silicon on 5GHz

Table 1. Integrated Phase Noise Corresponding to Phase Noise from 250kHz to 40MHz

Phase noise in RMS	*0.5 degree*	*1.0 degree*	*1.5 degree*
IPN (dBc)	-50	-44	-40.5

3. Numerical Analysis for ICI

3.1. ICI caused by Common Phase Error and Residual Frequency Offset Affiliations

In time domain, the received signal x_n at the nth sample can be represented as below:

$$x_n = \frac{1}{N}\sum_{k=0}^{N-1} A_k H_k e^{j\frac{2\pi kn}{N}} + w_n \tag{3}$$

where A_k is the modulated data, H_k represents the channel coefficient affecting subcarrier k, w_n is the samples of a zero-mean Gaussian noise process.

In a similar way, the received signal Y_k in frequency domain of sub-carrier k can be expressed as below:

$$\mathrm{Y}_k = \sum_{n=0}^{N-1} x_n\, e^{-j\frac{2\pi nk}{N}} e^{j\phi(n)} \tag{4}$$

where $\phi(n)$ denotes common phase error. Using above two equations, Y_k can be derived as below:

$$\mathbf{Y}_{\boldsymbol{k}} = \frac{\mathbf{1}}{\boldsymbol{N}}\sum_{\boldsymbol{n}=\mathbf{0}}^{\boldsymbol{N}-\mathbf{1}}\left\{\left\{\sum_{\boldsymbol{m}=\mathbf{0}}^{\boldsymbol{N}-\mathbf{1}}\boldsymbol{A}_{\boldsymbol{m}}\boldsymbol{H}_{\boldsymbol{m}}\boldsymbol{e}^{\boldsymbol{j}\frac{\mathbf{2}\boldsymbol{\pi}\boldsymbol{m}\boldsymbol{n}}{\boldsymbol{N}}}\right\}\boldsymbol{e}^{\boldsymbol{j}\boldsymbol{\phi}(\boldsymbol{n})}\right\}\boldsymbol{e}^{-\boldsymbol{j}\frac{\mathbf{2}\boldsymbol{\pi}\boldsymbol{k}\boldsymbol{n}}{\boldsymbol{N}}} + \boldsymbol{W}_{\boldsymbol{k}} \tag{5}$$

$$= \boldsymbol{A}_{\boldsymbol{k}}\boldsymbol{H}_{\boldsymbol{k}}\frac{\mathbf{1}}{\boldsymbol{N}}\sum_{\boldsymbol{n}=\mathbf{0}}^{\boldsymbol{N}-\mathbf{1}}\boldsymbol{e}^{\boldsymbol{j}\boldsymbol{\phi}(\boldsymbol{n})} + \frac{\mathbf{1}}{\boldsymbol{N}}\sum_{\boldsymbol{n}=\mathbf{0}}^{\boldsymbol{N}-\mathbf{1}}\sum_{\substack{\boldsymbol{m}=\mathbf{0}\\ \boldsymbol{m}\neq\boldsymbol{k}}}^{\boldsymbol{N}-\mathbf{1}}\boldsymbol{A}_{\boldsymbol{m}}\boldsymbol{H}_{\boldsymbol{m}}\boldsymbol{e}^{\boldsymbol{j}\frac{\mathbf{2}\boldsymbol{\pi}\boldsymbol{n}(\boldsymbol{m}-\boldsymbol{k})}{\boldsymbol{N}}}\boldsymbol{e}^{\boldsymbol{j}\boldsymbol{\phi}(\boldsymbol{n})} + \boldsymbol{W}_{\boldsymbol{k}}$$

where W_k is the sample of a zero-mean Gaussian noise process in frequency domain.

The first term on the r.h.s of (5) rotates the useful component $A_k H_k$ of each subcarrier by an equal amount and is independent of the particular sub-carrier. This is commonly known as the common phase error. The second term of (5) is the inter-carrier interference (ICI) caused by contributions from all subcarriers $m \neq k$ on k due to the loss of orthogonality. Let denote the ICI components as $\mathrm{Y}_{ICI,k}$.

To simplify the formula, $\phi(n)$ can be represented with residual frequency error $\varepsilon = \Delta f \cdot T_s$ and colored Gaussian phase noise $\varphi(n)$ as below:

$$\phi(n) = \frac{2\pi n\varepsilon}{N} + \varphi(n) \tag{6}$$

And, if $\varphi(n)$ is sufficiently small, it can be simplified as follows:

$$e^{j\varphi(n)} \approx 1 + j\varphi(n), \varphi(n) \ll 1 \tag{7}$$

Using this assumption, the ICI component $\mathrm{Y}_{ICI,k}$ can be divided into two ICI terms, $\mathrm{Y}_{ICI,\varepsilon,k}, \mathrm{Y}_{ICI,\varphi,k}$ as below:

$$\begin{aligned}
\mathrm{Y}_{ICI,k} &= \frac{1}{N}\sum_{n=0}^{N-1}\sum_{\substack{m=0\\ m\neq k}}^{N-1} A_m H_m e^{j\frac{2\pi n(m-k)}{N}} e^{j\left(\frac{2\pi n\varepsilon}{N}+\varphi(n)\right)} \\
&\approx \frac{1}{N}\sum_{n=0}^{N-1}\sum_{\substack{m=0\\ m\neq k}}^{N-1} A_m H_m e^{j\frac{2\pi n(m-k)}{N}} e^{j\frac{2\pi n\varepsilon}{N}} \cdot \big(1 + j\varphi(n)\big) \\
&= \frac{1}{N}\sum_{n=0}^{N-1}\sum_{\substack{m=0\\ m\neq k}}^{N-1} A_m H_m e^{j\frac{2\pi n(m-k)}{N}} e^{j\frac{2\pi n\varepsilon}{N}} \\
&\qquad + j\frac{1}{N}\sum_{n=0}^{N-1}\sum_{\substack{m=0\\ m\neq k}}^{N-1} A_m H_m e^{j\frac{2\pi n(m-k)}{N}} \varphi(n) \\
&= \mathrm{Y}_{ICI,\varepsilon,k} + \mathrm{Y}_{ICI,\varphi,k}
\end{aligned} \tag{8}$$

In following sub-chapters, these two ICI terms will be analysis in detail.

3.2. ICI caused by Residual Frequency Offset

The ICI caused by residual frequency offset can be represented as below:

$$
\begin{aligned}
Y_{ICI,\varepsilon,k} &= \frac{1}{N}\sum_{n=0}^{N-1}\sum_{\substack{m=0\\ m\neq k}}^{N-1} A_m H_m e^{j\frac{2\pi n(m-k)}{N}} e^{j\frac{2\pi n\varepsilon}{N}} \\
&= \sum_{\substack{m=0\\ m\neq k}}^{N-1} A_m H_m \frac{\sin(\pi\varepsilon)\cdot e^{\frac{j\pi\varepsilon(N-1)}{N}} e^{\frac{j\pi(m-k)}{N}}}{N\cdot\sin(\pi(m-k+\varepsilon)/N)}
\end{aligned} \tag{9}
$$

For simplicity of notation, it is assumed that the average channel gain is normalized to 1, i.e., $E[|H_m|^2] = 1$ in each subcarrier, and the transmitted symbols are of zero mean, *i.e.*, $E[|A_m|] = 0$, mutually uncorrelated per subcarrier, and of unit energy, *i.e.*, $E[|A_m A_k^*|] = \delta_{mk}$, where δ denotes the Kronecker delta function. Then, the variance of ICI caused by residual frequency offset at the kth subcarrier can be written as below:

$$
E\left[\left|Y_{ICI,\varepsilon,k}\right|^2\right] \leq \sum_{\substack{m=0\\ m\neq k}}^{N-1}\left(\frac{\sin(\pi\varepsilon)}{N\cdot\sin\left(\frac{\pi(m-k+\varepsilon)}{N}\right)}\right)^2 \tag{10}
$$

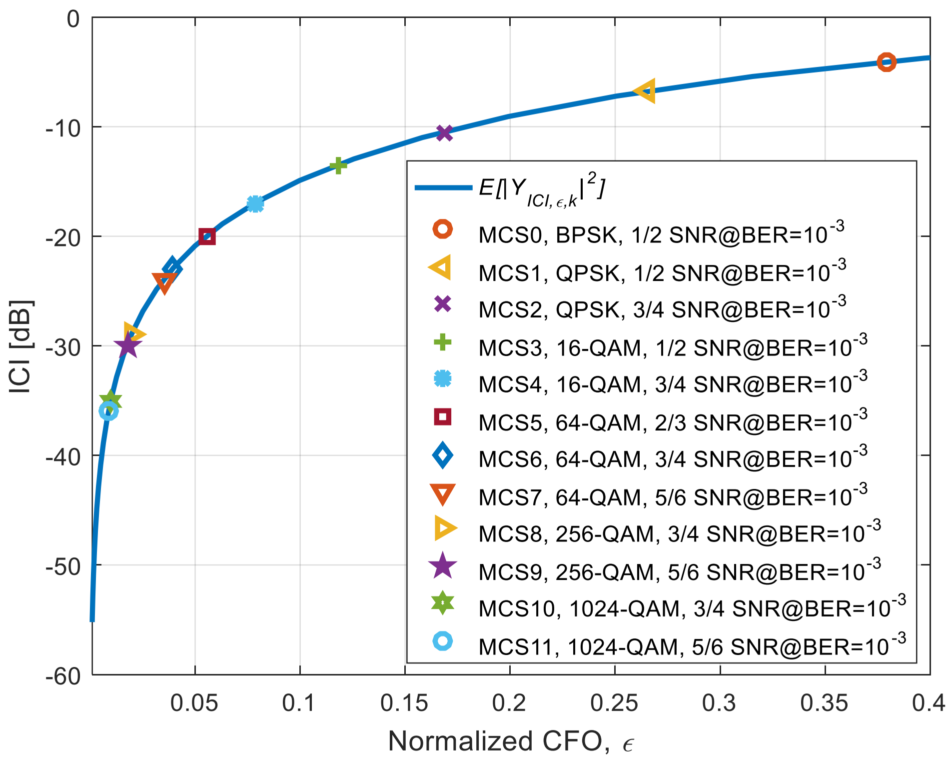

Figure 4. The Estimated ICI caused by Residual Frequency Offset and Required SNR per MCS on IEEE802.11ax and AWGN

Figure 4 shows the ICI predictions for residual frequency offset in (10). In addition, the AWGN environment of IEEE802.11ax analysed in [11] also shows the required SNR for each MCS. It is shown that the normalized carrier frequency ratio ε should be at least 0.0088 in order to satisfy 10^{-3} BER using MCS11 having 1024-QAM and 5/6 coding rate. Also, according to the carrier frequency offset correction method in [10], the standard deviation of the residual frequency offset is about 0.7kHz at 20MHz bandwidth and 5dB SNR. The expected value of $\left|\mathrm{Y}_{ICI,\varepsilon,k}\right|^2$ in this condition is less than -47.8dB. Therefore, ICI due to residual frequency offset can be neglected.

$$E\left[\left|\mathrm{Y}_{ICI,\varepsilon,k}\right|^2\right]\Big|_{\varepsilon=0.00224} \leq= -47.8\ \mathrm{dB} \tag{11}$$

where $\varepsilon = \Delta f \cdot \mathrm{T_s}$.

3.3. ICI caused by Common Phase Error

ICI term of (7) caused by common phase error, $\mathrm{Y}_{ICI,\varphi,k}$, can be rewritten as below:

$$E\left[\left|Y_{ICI,\varphi,k}\right|^2\right] = \left|\frac{1}{N}\sum_{n=0}^{N-1}\sum_{\substack{m=0\\ m\neq k}}^{N-1} A_m H_m e^{j\frac{2\pi n(m-k)}{N}}\varphi(n)\right|^2 \tag{12}$$

Under assuming the average channel gain is normalized to 1, *i.e.*, $E[|H_m|^2] = 1$ in each subcarrier, and the transmitted symbols are of zero mean, *i.e.*, $E[|A_m|] = 0$, it can be simplified as below:

$$\begin{aligned}
E\left[\left|Y_{ICI,\varphi,k}\right|^2\right] &\approx E\left[\left|\frac{1}{N}\sum_{n=0}^{N-1}\sum_{\substack{m=0\\ m\neq k}}^{N-1} e^{j\frac{2\pi n(m-k)}{N}}\varphi(n)\right|^2\right] \\
&= E\left[\left|\frac{1}{N}\sum_{n=0}^{N-1}\left(-1+\sum_{m=0}^{N-1} e^{j\frac{2\pi n(m-k)}{N}}\right)\varphi(n)\right|^2\right] \\
&= E\left[\left|\frac{1}{N}\sum_{n=0}^{N-1}\left(-1+N\delta(n)e^{-j2\pi nk}\right)\varphi(n)\right|^2\right] \\
&= E[\varphi(0)^2] - \frac{2}{N}\sum_{n=0}^{N-1}E[\varphi(0)\varphi(n)] + \frac{1}{N^2}E\left[\left(\sum_{n=0}^{N-1}\varphi(n)\right)^2\right] \\
&= R_\varphi(0) - \frac{2}{N}\sum_{n=0}^{N-1}R_\varphi(n) + \frac{1}{N^2}\left[N\cdot R_\varphi(0) + \sum_{m=1}^{N-1}\sum_{n=1}^{m}R_\varphi(n)\right]
\end{aligned} \tag{13}$$

Based on the one pole phase noise model in (1), the ICI power can be derived as:

$$E\left[\left|Y_{ICI,\varphi,k}\right|^2\right] \approx \sigma_\varphi^2\left[1-\frac{2}{N}\cdot\frac{1-a^N}{1-a}+\frac{1}{N}+\frac{2}{N}\cdot\frac{a}{1-a}-\frac{1}{N^2}\cdot\frac{a-a^{N+1}}{(1-a)^2}\right] \tag{14}$$

where σ_φ^2 is given by:

$$\sigma_\varphi^2 = \left(\frac{\pi}{180}n_{p,degree}\right)^2 \tag{15}$$

and a is given by:

$$a = \frac{1}{1 + 2\pi f_{3dB} T_s} \tag{16}$$

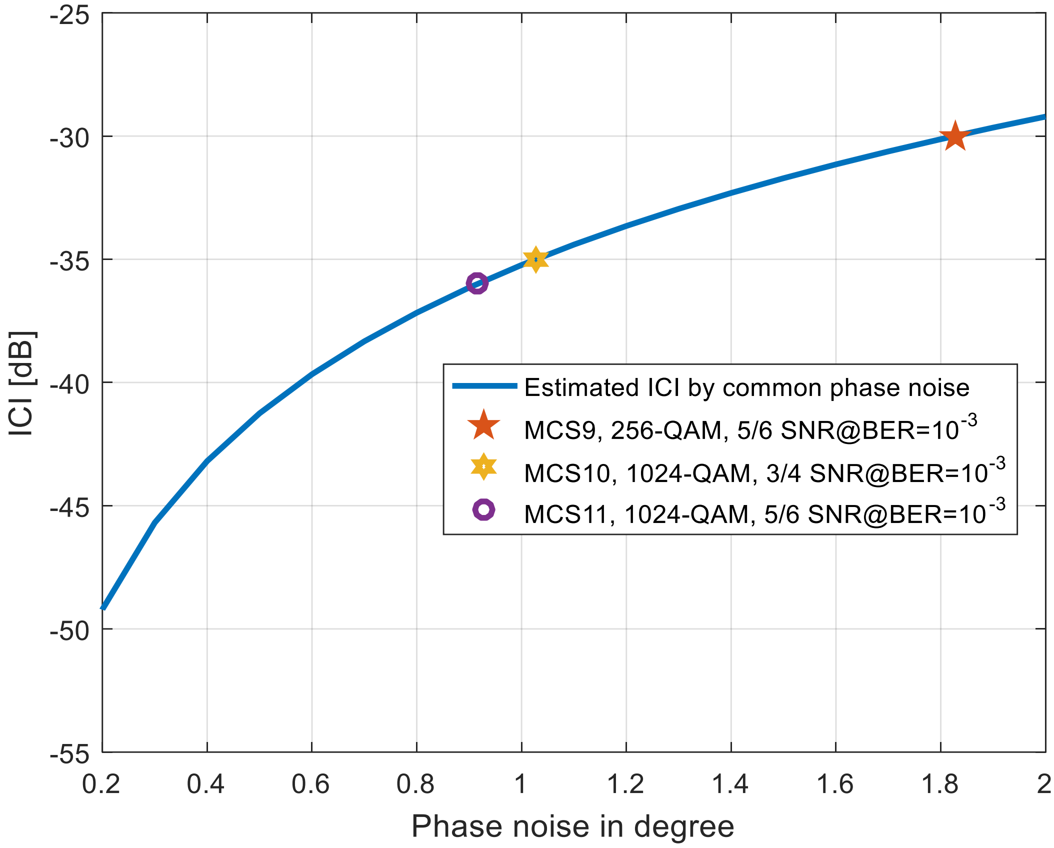

Figure 5. The Estimated ICI caused by Residual Frequency Offset and Required SNR per MCS on IEEE802.11ax and AWGN

Figure 5 shows the ICI predictions for the common phase noise expressed in (14), (15), and (16). Also, the required SNR for each MCS in the AWGN environment of IEEE802.11ax analyzed in [11] is also included. Assuming AWGN environment, it can be seen that the common phase noise should be below 0.92 ° in order for MCS11 to satisfy BER 10^{-3}. In the indoor environment (IEEE channel model D), assuming that the required SNR margin is about 6dB, the common phase noise should be less than 0.6˚. Therefore, it can be seen that ICI due to common phase noise is not cannot be ignored in order to satisfy 1024-QAM communication.

4. Conclusions

In this paper, to analyze ICI for closed-loop phase noise in OFDM communication system, phase noise model is verified based on measured phase noise, and based on this, we analyzed the interference between the residual frequency offset and the subcarrier by phase noise. Also, the maximum phase noise and residual frequency offset for the 10^{-3} BER are plotted by comparing the analyzed ICI components to the required SNR for each modulation order of IEEE802.11ax. As a result of the analysis, it is shown that ICI by phase noise is larger by 12.3dB in a general WLAN system than that by a residual frequency offset for a received signal having a 20MHz bandwidth, 5dB SNR and 1 degree phase noise.

Acknowledgments

This study was supported by research funding of the University of Osan in 2017.

References

[1] IEEE Computer Society, "Wireless LAN medium access control (MAC) and physical layer (PHY) specifications: Enhancements for very high throughput for operation in bands below 6 GHz", IEEE P802.11ac/D1.0 Std., **(2011)**.
[2] V. S. Abhayawardhana and I. J. Wassell, "Frequency scaled time domain equalization for OFDM in broadband fixed wireless access channels", Proceedings of the IEEE Wireless Communications and Networking Conference, **(2002)**.
[3] L. Piazzo and P. Mandarini, "Analysis of phase noise effects in OFDM modems", IEEE Trans. Commun., vol. 46, no. 10, **(2002)**, pp. 1696–1705.
[4] T. C. W. Schen, R. W. van der Hofstad, E. R. Fledderus and P. F. M. Smulders, "Distribution of the ICI term in phase noise impaired OFDM systems", IEEE Trans. Wireless Commun., vol. 6, no. 4, **(2007)**, pp. 1488–1500.
[5] P. Mathecken, T. Riihonen, S. Werner and R. Wichman, "Performance analysis of OFDM with Wiener phase noise and frequency selective fading channels", IEEE Trans. Commun., vol. 59, no. 5, **(2011)**, pp. 1321–1331.
[6] S. Stefanatos, F. Foukalas and T. Khattab, "On the Achievable Rates of OFDM with Common Phase Error Compensation in Phase Noise Channels", IEEE Trans. Commun., vol. 1, iss.99, **(2017)**.
[7] V.S. Abhayawardhana and I.J. Wassell, "Common Phase Error Correction for OFDM in Wireless Communication", GLOBECOM'02, **(2002)**.
[8] Maxim Integrated, MAX2828, MAX2829-Single-/Dual-Band 802.11a/b/g World-Band Transceiver ICs, https://datasheets.maximintegrated.com/en/ds/MAX2828-MAX2829.pdf, **(2015)**.
[9] M. Webster and M. Seals, "Suggested phase noise model for 802.11hrb", https://mentor.ieee.org/802.11/dcn/00/11-00-0296-01-00sb-suggested-phase- noise-model-for-802-11-hrb.ppt.
[10] Y. Yong, J. Haifang, F. Zhi and S. Yin, "The Frequency Offset Estimation and Tracking in MIMO-OFDM BASED 802.11n System", Procceding of International Conference on Networks Security, Wireless Comunications and Trusted Computing, vol. 1, **(2009)**, pp. 754-757.

Author

Jihun Koo, he received the B.S and M.S. degrees in Electrical Engineering from Inha University, Incheon, Korea, in 2000 and 2002, respectively and the Ph.D. degree from Yonsei University, Seoul, Korea in 2015. He was Principal engineer of Connectivity development team of Samsung Electronics Co., Ltd., Hwaseung, Gyeongi-do, Korea. He is currently a Professor in the Smart IT Department at Osan University, Osan, Korea. His current research interests include wireless communication, Internet-of-Things and Connectivity.

